Vol. 78: 249–259, 2019
https://doi.org/10.3354/cr01573

CLIMATE RESEARCH
Clim Res

Tropical cyclone frequency inferred from intra-annual density fluctuations in longleaf pine in Florida, USA

Tyler J. Mitchell[1,*], Paul A. Knapp[1], Jason T. Ortegren[2]

[1]Carolina Tree-Ring Science Laboratory, Department of Geography, Environment, and Sustainability,
University of North Carolina at Greensboro, PO Box 26170, Greensboro, NC 27402, USA
[2]Department of Earth and Environmental Sciences University of West Florida, 11000 University Pkwy, Pensacola, FL 32514, USA

ABSTRACT: We present a new method for identifying historic tropical cyclone activity utilizing frequencies of intra-annual density fluctuations in longleaf pine in western Florida. In addition, in this work we provide information about the causal factors that determine the formation of intra-annual density fluctuations (IADFs) in longleaf pine latewood. Specifically, we test the viability of using late latewood (L+) IADFs in longleaf pine as a proxy for historic tropical cyclone frequency and precipitation for the period 1950–2017. The stabilized frequency of L+ IADF occurrence is significantly ($p < 0.01$) associated with the Palmer drought severity index (PDSI) for the months June through October, indicating that high amounts of late growing-season moisture promote the formation of IADFs in latewood. We find the strongest relationships between PDSI and IADF occurrence during September and October, indicating the influence of tropical cyclone (TC)-sourced precipitation on IADF formation. High IADF stabilized frequencies (i.e. >0.50) nearly always (88%) coincide with a TC tracking into the study area, and we find a significant ($p < 0.01$) relationship between TC-sourced precipitation and the stabilized frequency of L+ IADFs. Via this relationship, reconstruction of historic tropical cyclone frequency and precipitation is probable, which would allow for increased understanding of historic tropical cyclone activity prior to the historic climate record.

KEY WORDS: Tropical cyclone · Intra-annual density fluctuation · Dendroclimatology · Florida · Longleaf pine

1. INTRODUCTION

Longleaf pine *Pinus palustris* Mill. is a long-lived (>400 yr) tree species found in the Atlantic and Gulf coastal plains from eastern Texas to Virginia (Burns & Honkala 1990, Frost 2007). The species was once the dominant pine of the coastal plains but has since declined in range from approximately 37 million to 1.75 million hectares due to anthropogenic influences including deforestation, fire suppression, and land-use changes (Frost 1993, 2007, Van Lear et al. 2005, Brockway et al. 2007, Oswalt et al. 2012, McIntyre et al. 2018). Longleaf pine is classified as a sturdy tree, likely due to a high heartwood-to-sapwood ratio (hence its historical use for ship masts), and the resin-laden tree is wind firm to hurricane-force winds (Gaby 1985, Conner et al. 1994, Provencher et al. 2001), yet highly dependent upon tropical cyclone precipitation (Knapp et al. 2016).

Climate-tree growth relationships for longleaf pine are well understood (Lodewick 1930, Coile 1936, Schumacher & Day 1939, Devall et al. 1991, Meldahl et al. 1999, Henderson & Grissino-Mayer 2009, Knapp et al. 2016, Mitchell et al. 2019). Generally, sufficient

---

*Corresponding author: tjmitche@uncg.edu

warm season current- and prior-year precipitation, including tropical cyclone precipitation, and cooler summer temperatures, are associated with increased radial growth in longleaf pine in Alabama (Meldahl et al. 1999), Florida (Lodewick 1930, Schumacher & Day 1939, Henderson & Grissino-Mayer 2009), Georgia (Coile 1936), Mississippi (Devall et al. 1991), North Carolina (Knapp et al. 2016, Patterson et al. 2016, Mitchell et al. 2019), South Carolina (Henderson & Grissino-Mayer 2009), and Texas (Henderson & Grissino-Mayer 2009).

Interannual ring-width variations in longleaf pine latewood are high for a species growing in mesic climates (e.g. Henderson & Grissino-Mayer 2009, Knapp et al. 2016, Mitchell et al. 2019) with mean sensitivities, which indicate year-to-year variability, matching that of species found in semiarid environments of the American West (e.g. Knapp et al. 2001). High sensitivity to mid-to-late summer precipitation may be a result of site preferability to sandy, well-drained soils, yet high mean sensitivity values found with longleaf pine growing in the well-developed, humus-rich loamy soils of the North Carolina piedmont (Mitchell et al. 2019) suggests the species may also be particularly in-tune with summer precipitation amounts regardless of local environmental conditions.

Here, we present a proxy method for identifying historic tropical cyclone (TC) activity utilizing frequencies of intra-annual density fluctuations (IADFs) in tree rings sampled from longleaf pine in western Florida. In addition, we provide information about the causal factors that determine the formation of IADFs in longleaf pine latewood. We also examine the potential El Niño-Southern Oscillation (ENSO) influence on IADF formation, as previous work indicates an influence of ENSO variability on precipitation regimes in the southeastern USA (Rajagopalan et al. 2000, Mo & Schemm 2008, Wang et al. 2010), though the influence is spatially and seasonally dependent, and appears to have been non-stationary during the 20th century (Rajagopalan et al. 2000, Mo & Schemm 2008, Seager et al. 2009, Wang et al. 2010, Li et al. 2013). Additionally, at interannual time scales, 20th century ENSO variability has been linked to variability in TC landfall probability and TC rainfall totals in the Southeast (Bove et al. 1998, Xie et al. 2005, Kossin et al. 2010, Colbert & Soden 2012).

1.1. Intra-annual density fluctuations (IADFs)

Longleaf pine has a high frequency of radial-growth anomalies including false and missing rings (Henderson & Grissino-Mayer 2009), suggesting that the temporal inconsistency of TC-derived precipitation that modulates latewood growth (Knapp et al. 2016) may be recorded in the ring widths as intra-annual density fluctuations (IADFs). IADFs (Fig. 1) are defined as anomalous variations in wood density, where earlywood- (latewood-)like cells are present within latewood (earlywood) (Fritts 1976).

Types of IADFs are classified based upon where the anomalous growth occurs relative to the annual growth ring (Campelo et al. 2007) as follows: Type E, latewood-like cells within earlywood; Type E+, 'transition' cells within earlywood to latewood; Type L, earlywood-like cells within latewood; and Type L+, earlywood-like cells between latewood and the earlywood of the next annual ring (Campelo et al. 2007) (Fig. 1). Here, we focus on IADFs found in longleaf latewood growth as latewood variations are more climatically sensitive than either earlywood or totalwood (Lodewick 1930, Meldahl et al. 1999, Henderson & Grissino-Mayer 2009, Knapp et al. 2016, Patterson et al. 2016). Specifically, we examine L+ types of IADFs as their location within latewood corresponds with late-summer precipitation, which is when longleaf pine is typically most stressed by soil-moisture deficiencies.

Much of the work that has examined IADF formation has been based on tree species native to the Mediterranean region and western Europe including

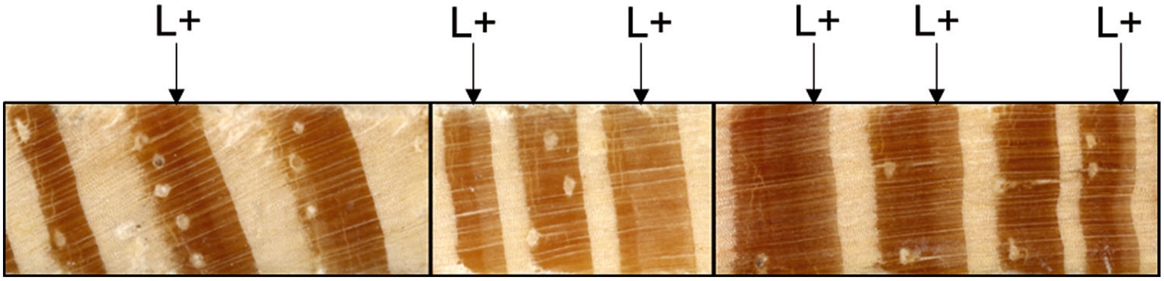

Fig. 1. Examples of 6 late latewood (L+) intra-annual density fluctuations (IADFs) from 3 samples of longleaf pine trees sampled for this study. An L+ IADF is characterized by less dense (thus lighter) cells at the end of the latewood (i.e. darker) band

Aleppo pine *P. halepensis* (de Luis et al. 2011a,b, Novak et al. 2013, Zalloni et al. 2016), maritime pine *P. pinaster* (Vieira et al. 2009, 2010, Rozas et al. 2011, Campelo et al. 2015, Zalloni et al. 2016), Scots pine *P. sylvestris* (Rigling et al. 2002), and stone pine *P. pinea* (Campelo et al. 2007, Zalloni et al. 2016). Conversely, only a few studies have worked with North American tree species (Schulman 1938, Copenheaver et al. 2006, Edmondson 2010, Marchand & Filion 2012) and to our knowledge, no North American study has examined IADFs in latewood.

Several factors may regulate IADF occurrence (Battipaglia et al. 2016). Tree age and IADF frequency are inversely related in multiple species of *Pinus* such that IADFs occur more frequently in younger individuals (Copenheaver et al. 2006, Vieira et al. 2009, 2010, Campelo et al. 2015, Zalloni et al. 2016). The relationship between tree age and IADF frequency is likely due to younger trees generally having longer growing seasons and a faster response to climatic conditions (Vieira et al. 2009). Additionally, a relationship between IADF occurrence and total tree-ring width has been reported, indicating that wider rings exhibit a higher frequency of IADFs compared to narrower, suppressed rings (Copenheaver et al. 2006, Campelo et al. 2013, Zalloni et al. 2016).

Climate and weather conditions have a significant influence and control on IADF formation. Previous investigations (Schulman 1938, Rigling et al. 2002, Campelo et al. 2007, Vieira et al. 2009, 2010, Edmondson 2010, de Luis et al. 2011a, Rozas et al. 2011, Palakit et al. 2012, Zalloni et al. 2016) report that IADFs present in earlywood (types E and E+) are generally linked to anomalous and unseasonal precipitation and temperature regimes in spring and early summer while IADFs present in latewood (types L and L+) are generally linked to either unseasonal precipitation or temperature regimes during late summer and fall. Thus, improved soil moisture conditions temporarily trigger the production of less-dense cell walls (i.e. producing the lighter wood, Fig. 1) during this period of favorable conditions. The relationship between climate and IADF formation allows for climate reconstructions to be produced at intra-seasonal resolution and the synchronistic occurrence of IADFs between individual trees and chronologies confirms the external sourcing of the triggering mechanism. For example, L+ IADFs may suggest above average precipitation in late summer and early fall. Additional research focused on *Pinus* species outside of the areas where IADF research has been prevalent (Battipaglia et al. 2016) has the potential to increase understanding of IADF formation and potentially create the ability to reconstruct intra-seasonal climatic anomalies in the region. Specifically, the examination of IADF frequency for longleaf pine will help establish if similar growth anomalies exist within the *Pinus* genus beyond the Mediterranean region and under a climatic regime characterized by wet (i.e. >5 cm rainfall per month) summers.

1.2. Longleaf pine latewood as a tropical cyclone precipitation proxy

Multiple proxy measures exist to reconstruct TC activity using longleaf pine tree-ring data (Miller et al. 2006, Lewis et al. 2011, Knapp et al. 2016, Labotka et al. 2016). Based on samples collected in North Carolina, Knapp et al. (2016) found variations in latewood ring-width had high fidelity ($r = 0.71$, $p < 0.01$) with tropical cyclone precipitation (TCP) and reconstructed annual TCP amounts during the last 200 yr. Variations in $\delta^{18}O$ isotope in longleaf pine latewood have also effectively documented historic TC frequency in southern Georgia (Miller et al. 2006, Labotka et al. 2016) and southeastern Texas (Lewis et al. 2011).

Here we present a dendroclimatic proxy measure that may effectively detect TC frequency and precipitation in the southeastern USA. We specifically examine the potential diagnostic role of L+ IADFs as a marker to identify the passage of TCs in western Florida. We then discuss how these findings could be applied to other areas of the southeastern USA as a proxy method of identifying TC passage prior to historic record keeping.

2. MATERIALS AND METHODS

2.1. Study sites

We analyzed IADF occurrence in longleaf pine at 3 field sites in the Gulf Coastal Plain of western Florida (Fig. 2). The selected sites (Naval Live Oaks Reservation [NLO], Blackwater River State Park [BRP], Blackwater River State Forest [BRF]) are in an area where the climatic influence of the Gulf of Mexico and TCs occurs, which may increase the occurrence of IADFs. Warm Gulf of Mexico sea-surface temperatures (SSTs) supply the study areas with increased precipitation (severe and non-severe) and warmer temperatures (Molina et al. 2016). Previous investigations on IADF occurrence generally occur along tree populations with an oceanic influence, so sites

Fig. 2. Field collection sites: (1) Naval Live Oaks Reservation (NLO); (2) Blackwater River State Park (BRP); (3) Blackwater River State Forest (BRF)

were selected in part to increase comparability with previous work.

The study region is affected by several climatic features that may influence radial growth including winters with minimal (i.e. ≤2) days below subfreezing conditions and the influence of TC-induced heavy rainfall events. In addition, the study region is climatically dissimilar to Mediterranean Europe, as summer precipitation in the study region is a significant precipitation source, while in Mediterranean Europe summer precipitation is a minor source (e.g. approximately <10%) of total annual precipitation near Galicia and Valencia in Spain.

We selected the 3 sites based on potential climate and land-use management characteristics that may influence the frequency of IADFs, and thus suggest IADF frequency is affected by site conditions. NLO was selected because it is located immediately adjacent to the Gulf of Mexico and experiences moderated temperature extremes relative to the 2 inland sites that are 38 km (BRP) and 60 km (BRF) northeast of NLO. NLO is characterized by sandy soils (77% Lakeland sand and similar soils) while the inland sites are primarily composed of loamy sands and similar soils (85% Troup loamy sand). The coastal site is at an elevation of approximately 2 to 9 m, while the inland sites range from 12 to 41 m at BRP and from 30 to 62 m at BRF. Both BRP and BRF are more frequently burned than NLO, suggesting that land management is considerably different between sites.

Fig. 3. Open-canopy longleaf pine forest environment at Blackwater River State Forest. We sampled in open-canopy environments to reduce potential factors confounding radial growth

2.2. Longleaf pine tree-ring data

At each of the 3 field sites, we sampled 10 to 15 trees in open-canopy environments (Fig. 3), obtaining 2 core samples per tree (n = 20 to 30). We used a 5.15 mm diameter increment borer following standard dendrochronological field sampling techniques and sampled from south-facing slopes when possible, to maximize the climate signal contained in the latewood (Stokes & Smiley 1996). We recorded tree height, stem diameter, and geographic location for each tree. After field collection, core samples were dried, then mounted and glued onto wooden strips. Mounted cores were sanded with progressively finer sand paper ranging from 600 down to 120 µm to reveal cellular structure, scanned at high resolution (dots per inch [DPI] ≥ 1200) and tree-ring widths were measured using the program WinDENDRO™ at 0.001 mm precision (Guay 2012). Raw tree-ring widths were checked for accuracy using the program COFECHA to confirm crossdating (Holmes 1983). In addition, we tested multiple standardization techniques including basal area increment, negative exponential, and raw ring widths, and found the best correlations with climate using negative exponential standardization. We standardized each core's growth using negative exponential standardization to examine individual core sensitivity to climate.

2.3. IADFs

After crossdating we inspected each core for cellular-level radial growth anomalies and classified in agreement with previous investigations (Campelo et al. 2007). The frequency of IADFs per year (F) was calculated as $F = N / n$ where N is the number of IADFs each year and n is the total sample depth at that given year. The decreasing sample depth (n) through time potentially creates a bias which was corrected using an adjusted frequency equation (Osborn et al. 1997). The stabilized IADF frequency (f) was calculated using $f = Fn^{0.5}$.

2.4. Climate and weather data

Monthly climate data (e.g. Palmer drought severity index [PDSI], minimum temperature, maximum temperature, average temperature, and precipitation) for Climate Division 1 in northwest Florida were collected from the NOAA National Climate Data Center for the period 1950–2017 (www7.ncdc.noaa.gov/CDO/CDODivisionalSelect.jsp). For the same period, daily precipitation data were collected for the weather station at the Pensacola Regional Airport (Station ID: USW00013899; at most ~45 km from study areas) from the NOAA National Centers for Environmental Information (NCEI 2018) (www.ncdc.noaa.gov/data-access/land-based-station-data) to determine TCP. Additionally, we collected ENSO data for the 3.4 region from NOAA to determine the influence of ENSO on the frequency and formation of IADFs (https://www.esrl.noaa.gov/psd/gcos_wgsp/Timeseries/Nino34/). Lastly, because of its documented association with both precipitation variability (e.g. Ortegren et al. 2011, 2014) and regional TC landfall frequency (e.g. Ortegren & Maxwell 2014) in our study area, we computed the monthly Bermuda High Index (BHI; Stahle & Cleaveland 1992, Katz et al. 2003, Ortegren et al. 2014). We retrieved sea-level pressure data from the National Centers for Atmospheric Research (2019). The BHI is the standardized time series of differences in monthly average sea-level air pressure between Bermuda (35° N, 65° W) and New Orleans (30° N, 90° W), calculated as Bermuda minus New Orleans. Positive (negative) values of the BHI indicate periods of eastward (westward) displacement of the southerly airflow in the west flank of the Bermuda High. We computed the monthly BHI as well as multi-month averages to examine the possible relationship at both monthly and seasonal time scales.

2.5. Tropical cyclone data

To determine if a TC tracked into the study area, we examined historic TC tracks from the International Best Track Archive for Climate Stewardship (IBTrACS) (Knapp et al. 2010), excluding non-developing tropical depressions and subtropical cyclones (Landsea & Franklin 2013). To determine TC influence on the study area we used a 223 km (the average rain-field size at landfall) TC-moisture plume buffer radius for the months July, August, September, and October (Matyas 2010, Zhou & Matyas 2017). We excluded June and November, as a TC occurring in either of these months would likely not be picked up in the latewood of that year (Lodewick 1930). We collected TCP values for the days when a TC influenced the study area (i.e. tracked within 223 km of the study area) by attributing all same-day precipitation to the tropical system (Knapp et al. 2016).

2.6. Analyses

To determine if site-specific differences exist in L+ IADF occurrence, we used an analysis of variance (ANOVA) and Tukey-Kramer post-hoc procedures to determine if the mean L+ IADF occurrence at each site was significantly different. In addition, we tested the tree characteristics (i.e. age, diameter, height) at each study site to determine if there were significant site-specific differences in tree morphology and age.

We examined each core's relationship with climate to determine if the climate sensitivity of a tree contributes to a higher proportion of L+ IADFs during the common data period (1972–2017). We correlated each core's standardized growth with monthly PDSI, and used a Mann-Whitney U-test to determine if the group of cores that were significantly associated with climate were different from the group of cores with no significant relationship to climate regarding total L+ IADFs.

We tested the relationship between the stabilized frequency of IADF occurrence and climatic variables (monthly PDSI, TCP) using Spearman's rank-order correlation to determine the influence of summer precipitation on L+ IADF formation. We also tested whether a TC influenced the study region for each year that the stabilized frequency of IADF occurrence is >0. We examined climate (precipitation, ENSO, and ENSO phase) during the occurrence of non-TC positives (i.e. an L+ IADF in a year without TC influence) to determine what causes an L+ in the region in years with no TC influence.

3. RESULTS AND DISCUSSION

The final sample consisted of 34 trees (n = 67 cores) sampled from the 3 study sites (Fig. 4). L+ IADFs per sample ranged from 0 to 14, ($\sigma = 2.8$) during the common period of growth (1972–2017) indicating that certain trees are more effective at capturing L+ IADFs (Fig. 4). During the common period of growth (i.e. the range of years in which n = 67), BRF had the highest mean L+ events per year ($\bar{x} = 4.08$), followed by BRP ($\bar{x} = 2.95$), and NLO ($\bar{x} = 1.41$). The mean L+ IADFs per site were significantly different ($p = 0.003$), with more L+ IADFs at BRF than NLO, indicating that there were significant site-specific differences in the study region. In addition, we tested whether tree characteristics (i.e. age, diameter, height) were significantly different between sites and found that there were significant ($p < 0.001$) differences in both age and diameter between sites. BRP trees were significantly wider ($p < 0.05$) than BRF trees, which were significantly wider ($p < 0.05$) than NLO trees. In addition, we found that NLO trees were significantly older ($p < 0.05$) than BRF trees, and found no significant difference in cambial age between BRF and BRP.

These findings that older and smaller diameter trees (NLO) had fewer L+ IADFs agree with previous work (Copenheaver et al. 2006, Vieira et al. 2009, 2010, Campelo et al. 2015, Zalloni et al. 2016), suggesting that IADF formation is similar in both Mediterranean Europe and our study region. In addition, the role of land management should be accounted for when comparing site characteristics. Between these 3 study sites, the more maintained (i.e. with more frequent prescribed fires) sites (BRP and BRF) had more L+ IADFs than the less frequently burned site (NLO), which indicates the potential influence of land management on IADF formation. The open-canopy environments produced by frequent prescribed fires limit confounding factors on radial growth, which could explain the higher sensitivity to L+ IADFs in these environments.

Climate/radial growth sensitivity of the cores did not have a significant influence on L+ frequency during the common growth period of 1972–2017 (n = 67 cores). Approximately one-third (n = 23) of the samples were significantly ($p < 0.05$) correlated with September PDSI, with the remainder (n = 44) not significant, suggesting substantial intra-site climate sensitivity. Conversely, climate sensitivity did not confer a higher likelihood of L+ frequency as there was no significant difference between the samples with significant climate-growth relationships ($\bar{x} = 3.2$ L+ IADFs per sample) and those without ($\bar{x} = 2.7$).

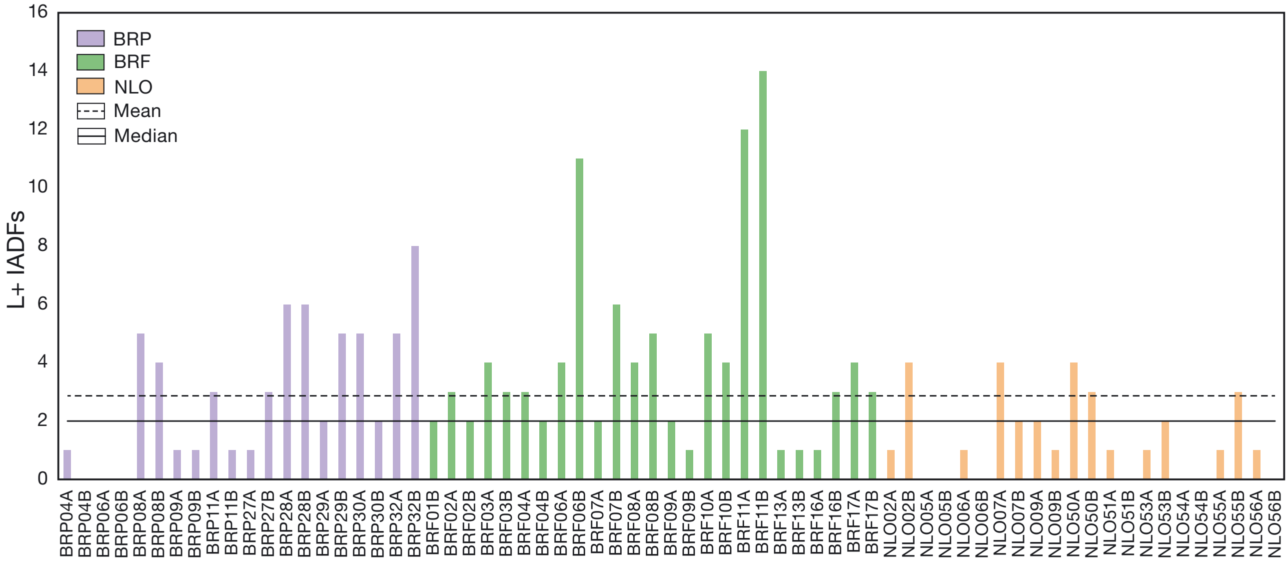

Fig. 4. Raw occurrence of L+ IADFs per sample at each site (Blackwater River State Park [BRP], n = 20; Blackwater River State Forest [BRF], n = 25; Naval Live Oaks Reservation [NLO], n = 22) during the common period of growth (1972–2017)

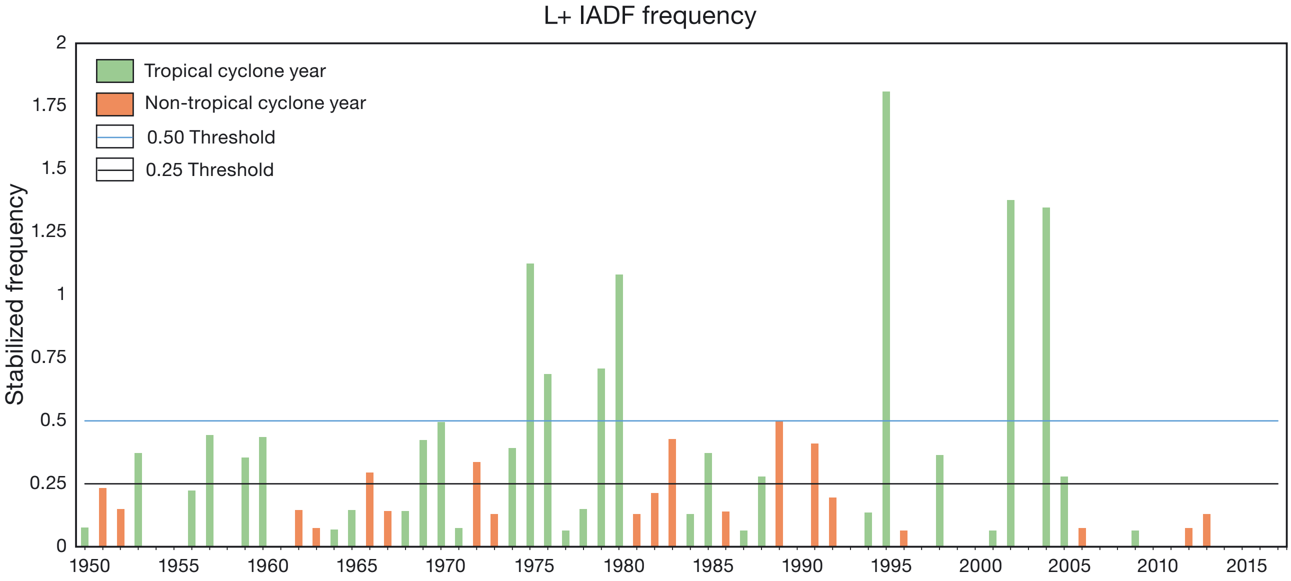

Fig. 5. The stabilized frequency, f, of L+ IADF occurrence. Seven of the 8 f-values > 0.5 from 1950–2017 correspond with a TC tracking into the study area during either July, August, September, or October. In addition, 14 of the 18 (78%) years with zero L+ IADF occurrence (no bar) are non-tropical cyclone years

The stabilized frequency (f) of L+ IADF occurrence (Fig. 5) was significantly associated ($p < 0.01$) with PDSI for the months June through October (Fig. 6). More late-season moisture associated with increased L+ IADF occurrence is in agreement with previous investigations (Rigling et al. 2002, Campelo et al. 2007, Vieira et al. 2009, 2010, de Luis et al. 2011a, Rozas et al. 2011, Zalloni et al. 2016), indicating that the causal mechanisms of IADFs are similar across study areas. The strongest relationships occurred in September and October, indicating the potential influence of TC-sourced precipitation on f, although we recognize this is also an artifact of L+ IADFs forming in the latter portion of latewood, which coincides with the second half of the TC season.

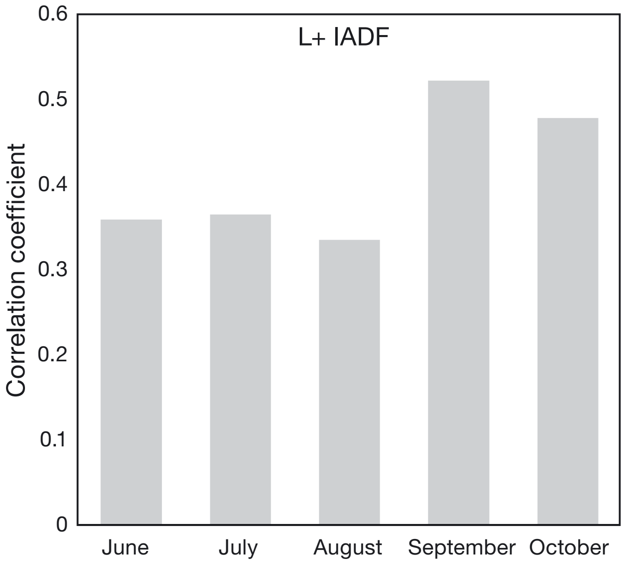

Fig. 6. Stabilized frequency of L+ IADF occurrence, f, is significantly associated ($p < 0.01$) with the Palmer drought severity index (PDSI) during each month from June to October

The specific influence of TC-sourced precipitation is likely the principal cause for the formation of L+ IADF in this region. During 1950–2017, 38 of the 68 years (56%) experienced a TC tracking within the study area. The type L+ f-values in years that had a TC track into the study area and the years that did not were significantly different ($p = 0.021$), indicating an influence of TC passage into the study area on stabilized L+ frequency (i.e. 'f'). Further, of the 50 years with $f > 0$, 31 (62%) were associated with TC passage while 19 (38%) were not, suggesting L+ events were an effective, but not an exclusive, marker of TC passage in the study area (Fig. 5). However, the majority (83%) of non-TC positives ($f > 0$, but no TC passage) occurred with $f < 0.25$. Conversely, for $f \geq 0.25$, 18 of the 23 years (78.26%) were associated with TC passage, while for $f \geq 0.50$, 7 of the 8 years (88%) were associated with TC passage indicating that L+ IADF may be an effective marker of historic TC passage when f is greater than a certain threshold (i.e. 0.25). In addition, there was no significant difference in total July–October precipitation between the years with an L+ IADF and TC (Group 1) and non-IADF/TC years (Group 2), suggesting that TCP is the primary cause of L+ IADFs. In the years with high f-values and no TC influence (orange bars in Fig. 5), we examined minimum and maximum temperature, precipitation, and PDSI during July–October and found no consistent pattern in these variables in these years. We posit that non-climatic individual-tree level growth releases might be occurring in these years.

Trees with a higher frequency of TC-coincident L+ IADFs were also more prone ($p < 0.01$) to record non-TC positives, suggesting that TC detection is partially an artifact of individual-level tree sensitivity. We found weak to non-existent associations between trees that had non-TC positives (i.e. an L+ IADF in a year without TC influence) and teleconnective patterns. Eighteen of the 34 trees in the sample had non-TC positives and there was a total of 55/387 (14%) incidents of non-TC positives. Significant ($p < 0.01$) differences existed between trees with non-TC positives and trees without non-TC positives in regard to each group's ability to capture a TC, such that the group of trees with non-TC positives were also more effective at identifying TCs. Despite a near-equal distribution of El Niño ($n = 25$), La Niña ($n = 22$) and neutral ($n = 21$) phases of the ENSO during the study period, most (47 of 55, 85%) non-TC positives coincided with either the El Niño or neutral phase ENSO. However, we found no significant relationship between ENSO and non-TC positives, with the strongest relationship occurring during June–August ($r = 0.172$, $p = 0.161$). In addition, we found no significant difference between the number of non-TC positives in a year depending on whether it was an El Niño or neutral year, suggesting that ENSO variability does not explain variations in non-TC positives. We found no significant relationship between June–October precipitation and non-TC positives, suggesting that non-TC positives could be caused by non-moisture based variables.

In contrast, there was a significant ($r = -0.255$, $p < 0.05$) correlation between non-TC positives and the July–October average BHI. This result suggests that a negative BHI (a 'westward' migration of the western ridge of the Bermuda High) during the TC season is associated with increased non-TC positives. Because negative BHI conditions are associated (at multidecadal time scales) with positive anomalies in both regional soil moisture (Ortegren et al. 2011, 2014) and Gulf Coast TC landfalls (Ortegren & Maxwell 2014), this finding indicates the possibility that increased seasonal (non-tropical) rainfall and increased TC landfalls (and thus TC rainfall) tend to coincide, and suggests that higher seasonal precipitation totals during the TC season (regardless of the rainfall source) may promote increased non-TC positives. However, we interpret this result with some caution, both because of the relative weakness of the statistical linkage and because of the contrasting findings regarding total rainfall and the frequency of non-TC positives.

The binary occurrence of a TC provides information regarding TC frequency while the magnitude of TCP could also explain variations in *f*. TCP and *f* were significantly associated ($p = 0.005$), yet the relationship explained only 15% of the total variance (Table 1). To examine the TCP and *f* relationship at a finer resolution, thresholds in the *f*-value were defined to determine if TCP becomes a more important explanatory variable at higher *f*-values.

When *f* was restricted to a threshold of ≥0.25, the relationship with TCP was insignificant, indicating that the initial correlation may have been an artifact of sample size rather than influence (i.e. significance without meaningful explanatory power). However, when *f* was restricted to values ≥0.50, these values were significantly associated with TCP ($p = 0.015$) (Table 1). TCP explained 65.6% of the variation in the $f \geq 0.50$ values. This indicates that L+ IADFs may only be an adequate diagnostic metric for historic TCP when the *f*-value exceeds a certain threshold (i.e. 0.50). Additionally, these results indicate that L+ IADFs may be an effective marker of TC passage, but an ineffective marker of the magnitude of TCP produced by a TC. It is likely that the width of an L+ IADF may be a more effective marker of TCP, while the occurrence of an L+ IADF may be a more effective marker of TC frequency.

These results indicate that L+ IADFs are an effective marker of historic TC frequency for the period 1950–2017, providing another proxy method to identify TC occurrence (cf. Miller et al. 2006, Lewis et al. 2011, Knapp et al. 2016, Labotka et al. 2016, Tucker et al. 2018). Collecting more samples from older trees and/or remnant stumps, which are plentiful in the southeastern USA (e.g. Henderson & Grissino-Mayer 2009), has the potential to examine the proxy relationship further and potentially extend the record of historic TC frequency beyond historic climate re-

Table 1. Spearman's rank correlation coefficient (r_S) values between *f*-values and tropical cyclone precipitation (TCP) totals during 1950–2017. *$p < 0.05$; **$p < 0.01$

f-value threshold	n	Correlation coefficient
None	68	0.353**
$f \geq 0.25$	23	0.188
$f \geq 0.50$	8	0.810*

cords at this location. This method also has the potential to reconstruct historic TC frequency throughout the southeastern United States, resulting in comparisons to previous work to address spatiotemporal patterns of TC activity in the USA, which is based largely on TC data from the early 1900s to the present (Keim et al. 2007).

4. CONCLUSION

These results indicate that while any large precipitation event in the late growing season can promote L+ IADF occurrence, higher stabilized frequency values of L+ IADF indicate an increased probability that a TC tracked into the study area and reduce the odds of a non-TC positive (i.e. $f > 0$ but no TC passage). Positive f-values below a certain threshold (i.e. $f \leq 0.50$), however, are less diagnostic of the magnitude of TCP in a given year. Despite these promising findings, data from more sites and older trees are needed to support these results. Further, via this relationship, reconstruction of specific environmental phenomena (e.g. TC passage into a specific study area) is probable, which could allow for increased understanding of historic TC activity prior to the historic climate record. Previous research (e.g. Miller et al. 2006, Knapp et al. 2016) shows that longleaf pine trees record TCP in their latewood, and the method proposed in this work could act as an additional confirmatory metric of historic TC passage and precipitation.

Acknowledgements. We thank Christopher Landsea and 2 other anonymous reviewers for their constructively critical comments that significantly improved our manuscript. We also thank Don Kerrigan for field assistance and Dan Royall for comments on the original manuscript. Finally we thank the editor, Guoyu Ren, for his editorial suggestions.

LITERATURE CITED

Battipaglia G, Campelo F, Vieira J, Grabner M and others (2016) Structure and function of intra-annual density fluctuations: mind the gaps. Front Plant Sci 7:595

Bove MC, Elsner JB, Landsea CW, Niu X, O'Brien JJ (1998) Effect of El Niño on U.S. landfalling hurricanes, revisited. Bull Am Meteorol Soc 79:2477–2482

Brockway DG, Outcalt KW, Boyer WD (2007) Longleaf pine regeneration ecology and methods. In: Jose S, Jokela EJ, Miller DL (eds) The longleaf pine ecosystem. Springer Series on Environmental Management. Springer, New York, NY, p 95–133

Burns RM, Honkala BH (1990) Silvics of North America. Vol 1, Conifers. United States Department of Agriculture (USDA), Forest Service, Agriculture Handbook 654. Washington, DC

Campelo F, Nabais C, Freitas H, Gutiérrez E (2007) Climatic significance of tree-ring width and intra-annual density fluctuations in *Pinus pinea* from a dry Mediterranean area in Portugal. Ann For Sci 64:229–238

Campelo F, Vieira J, Nabais C (2013) Tree-ring growth and intra-annual density fluctuations of *Pinus pinaster* responses to climate: does size matter? Trees (Berl) 27: 763–772

Campelo F, Vieira J, Battipaglia G, de Luis M, Nabais C, Freitas H, Cherubini P (2015) Which matters most for the formation of intra-annual density fluctuations in *Pinus pinaster*: age or size? Trees (Berl) 29:237–245

Coile T (1936) The effect of rainfall and temperature on the annual radial growth of pine in the southern United States. Ecol Monogr 6:533–562

Colbert AJ, Soden BJ (2012) Climatological variations in North Atlantic tropical cyclone tracks. J Clim 25:657–673

Conner RN, Rudolph DC, Saenz D, Schaefer RR (1994) Heartwood, sapwood, and fungal decay associated with red-cockaded woodpecker cavity trees. J Wildl Manag 58:728–734

Copenheaver CA, Pokorski EA, Currie JE, Abrams MD (2006) Causation of false ring formation in *Pinus banksiana*: a comparison of age, canopy class, climate and growth rate. For Ecol Manage 236:348–355

de Luis M, Novak K, Raventós J, Gričar J, Prislan P, Čufar K (2011a) Climate factors promoting intra-annual density fluctuations in Aleppo pine (*Pinus halepensis*) from semiarid sites. Dendrochronologia 29:163–169

de Luis M, Novak K, Raventós J, Gričar J, Prislan P, Čufar K (2011b) Cambial activity, wood formation and sapling survival of *Pinus halepensis* exposed to different irrigation regimes. For Ecol Manage 262:1630–1638

Devall MS, Grender JM, Koretz J (1991) Dendroecological analysis of a longleaf pine *Pinus palustris* forest in Mississippi. Vegetatio 93:1–8

Edmondson JR (2010) The meteorological significance of false rings in eastern redcedar (*Juniperus virginiana* L.) from the southern Great Plains, USA. Tree-Ring Res 66: 19–33

Fritts H (1976) Tree rings and climate. Academic Press, New York, NY

Frost CC (1993) Four centuries of changing landscape patterns in the longleaf pine ecosystem. In: Hermann SM (ed) Proceedings of the tall timbers fire ecology conference, No. 18. The longleaf pine ecosystem: ecology, restoration and management. Tall Timbers Research Station, Tallahassee, FL, p 17–43

Frost CC (2007) History and future of the longleaf pine ecosystem. In: Jose S, Jokela EJ, Miller DL (eds) The longleaf pine ecosystem. Springer Series on Environmental Management. Springer, New York, NY, p 9–48

Gaby LI (1985) The southern pines, an American wood. US Department of Agriculture Forest Service, FS–256. Washington, DC

Guay R (2012) WinDENDRO 2012: user's guide. Regent Instruments, Quebec

Henderson JP, Grissino-Mayer HD (2009) Climate–tree growth relationships of longleaf pine (*Pinus palustris* mill.) in the Southeastern Coastal Plain, USA. Dendrochronologia 27:31–43

Holmes RL (1983) Computer-assisted quality control in tree-ring dating and measurement. Tree-Ring Bull 43:69–78

Katz RW, Parlange MB, Tebaldi C (2003) Stochastic modeling of the effects of large-scale circulation on daily weather in the Southeastern U.S. Clim Change 60:189–216

Keim BD, Muller RA, Stone GW (2007) Spatiotemporal patterns and return periods of tropical storm and hurricane strikes from Texas to Maine. J Clim 20:3498–3509

Knapp KR, Kruk MC, Levinson DH, Diamond HJ, Neumann CJ (2010) The international best track archive for climate stewardship (IBTrACS) unifying tropical cyclone data. Bull Am Meteorol Soc 91:363–376

Knapp PA, Soulé PT, Grissino Mayer HD (2001) Post drought growth responses of western juniper (*Juniperus occidentalis* var. *occidentalis*) in central Oregon. Geophys Res Lett 28:2657–2660

Knapp PA, Maxwell JT, Soulé PT (2016) Tropical cyclone rainfall variability in coastal North Carolina derived from longleaf pine (*Pinus palustris* Mill.): AD 1771–2014. Clim Change 135:311–323

Kossin JP, Camargo SJ, Sitkowski M (2010) Climate modulation of North Atlantic hurricane tracks. J Clim 23: 3057–3076

Labotka DM, Grissino-Mayer HD, Mora CI, Johnson EJ (2016) Patterns of moisture source and climate variability in the southeastern United States: a four-century seasonally resolved tree-ring oxygen-isotope record. Clim Dyn 46:2145–2154

Landsea CW, Franklin JL (2013) Atlantic hurricane database uncertainty and presentation of a new database format. Mon Weather Rev 141:3576–3592

Lewis DB, Finkelstein DB, Grissino-Mayer HD, Mora CI, Perfect E (2011) A multitree perspective of the tree ring tropical cyclone record from longleaf pine (*Pinus palustris* Mill.), Big Thicket National Preserve, Texas, United States. J Geophys Res Biogeosci 116:G02017

Li L, Li W, Barros AP (2013) Atmospheric moisture budget and its regulation of the summer precipitation variability over the southeastern United States. Clim Dyn 41:613–631

Lodewick JE (1930) Effect of certain climatic factors on the diameter growth of longleaf pine in western Florida. J Agric Res 41:349–363

Marchand N, Filion L (2012) False rings in the white pine (*Pinus strobus*) of the Outaouais Hills, Quebec (Canada), as indicators of water stress. Can J For Res 42:12–22

Matyas CJ (2010) Associations between the size of hurricane rain fields at landfall and their surrounding environments. Meteorol Atmos Phys 106:135–148

McIntyre RK, Guldin JM, Ettel T, Ware C, Jones K (2018) Restoration of longleaf pine in the southern United States: a status report. Proc 19th biennial southern silvicultural research conference, March 14–16 2017, Blacksburg, VA. e-Gen Tech Rep SRS-234. US Department of Agriculture, Forest Service, Southern Research Station, Asheville, NC, p 297–302

Meldahl R, Pederson N, Kush J, Varner J (1999) Dendrochronological investigations of climate and competitive effects on longleaf pine growth. In: Wimmer R, Vetter RE (eds) Tree ring analysis: biological, methodological and environmental aspects. CABI Publishing, Wallingford, p 265–285

Miller DL, Mora CI, Grissino-Mayer HD, Mock CJ, Uhle ME, Sharp Z (2006) Tree-ring isotope records of tropical cyclone activity. Proc Natl Acad Sci USA 103:14294–14297

Mitchell TJ, Patterson TW, Knapp PA (2019) Comparison of climate–growth responses of montane and piedmont longleaf pine (*Pinus palustris* Mill.) chronologies in North Carolina. Trees (Berl) 33:615–620

Mo KC, Schemm JE (2008) Relationships between ENSO and drought over the southeastern United States. Geophys Res Lett 35:L15701

Molina M J, Timmer RP, Allen JT (2016) Importance of the Gulf of Mexico as a climate driver for US severe thunderstorm activity. Geophys Res Lett 43:12295–12304

National Centers for Atmospheric Research (2019) CISL research data archive 2019. http://rda.ucar.edu/datasets/ds010.1/ (last accessed 21 June 2019)

National Centers for Environmental Information (NCEI) (2018) www.ncei.noaa.gov/access (accessed 10 August 2018)

Novak K, Sánchez MAS, Čufar K, Raventós J, de Luis M (2013) Age, climate and intra-annual density fluctuations in *Pinus halepensis* in Spain. IAWA J 34:459–474

Ortegren JT, Maxwell JT (2014) Spatiotemporal patterns of drought/tropical cyclone co-occurrence in the southeastern USA: linkages to North Atlantic climate variability. Geogr Compass 8:540–559

Ortegren JT, Knapp PA, Maxwell JT, Tyminski WP, Soulé PT (2011) Ocean–atmosphere influences on low-frequency warm-season drought variability in the Gulf Coast and southeastern United States. J Appl Meteorol Climatol 50: 1177–1186

Ortegren JT, Weatherall A, Maxwell JT (2014) Subregionalization of low-frequency summer drought variability in the southeastern United States. Prof Geogr 66:323–332

Osborn TJ, Biffa KR, Jones PD (1997) Adjusting variance for sample-size in tree-ring chronologies and other regional-mean timeseries. Dendrochronologia 15:89–99

Oswalt CM, Cooper JA, Brockway DG, Brooks HW and others (2012) History and current condition of longleaf pine in the southern United States. Gen Tech Rep SRS–166. US Department of Agriculture Forest Service, Southern Research Station Asheville, NC

Palakit K, Siripattanadilok S, Duangsathaporn K (2012) False ring occurrences and their identification in teak (*Tectona grandis*) in north-eastern Thailand. J Trop For Sci 24:387–398

Patterson TW, Cummings LW, Knapp PA (2016) Longleaf pine (*Pinus palustris* Mill.) morphology and climate/growth responses along a physiographic gradient in North Carolina. Prof Geogr 68:238–248

Provencher L, Litt AR, Gordon DR, LeRoy Rodgers H and others (2001) Restoration fire and hurricanes in longleaf pine sandhills. Ecol Restor 19:92–98

Rajagopalan B, Cook E, Lall U, Ray BK (2000) Spatiotemporal variability of ENSO and SST teleconnections to summer drought over the United States during the twentieth century. J Clim 13:4244–4255

Rigling A, Bräker O, Schneiter G, Schweingruber F (2002) Intra-annual tree-ring parameters indicating differences in drought stress of *Pinus sylvestris* forests within the Erico-Pinion in the Valais (Switzerland). Plant Ecol 163:105–121

Rozas V, García-González I, Zas R (2011) Climatic control of intra-annual wood density fluctuations of *Pinus pinaster* in NW Spain. Trees (Berl) 25:443–453

Schulman E (1938) Classification of false annual rings in Monterey pine. Tree-Ring Bull 4:4–7

Schumacher FX, Day BB (1939) The influence of precipitation upon the width of annual rings of certain timber trees. Ecol Monogr 9:387–429

Seager R, Tzanova A, Nakamura J (2009) Drought in the southeastern United States: causes, variability over the last millennium, and the potential for future hydroclimate change. J Clim 22:5021–5045

Stahle DW, Cleaveland MK (1992) Reconstruction and analysis of spring rainfall over the southeastern U.S. for the past 1000 years. Bull Am Meteorol Soc 73:1947−1961

Stokes MA, Smiley TL (1996) An introduction to tree-ring dating. University of Arizona Press, Tucson, AZ

Tucker CS, Trepanier JC, Harley GL, DeLong KL (2018) Recording tropical cyclone activity from 1909 to 2014 along the northern Gulf of Mexico using maritime slash pine trees (*Pinus elliottii* var. *elliottii* Engelm.). J Coast Res 34:328−340

Van Lear DH, Carroll W, Kapeluck P, Johnson R (2005) History and restoration of the longleaf pine-grassland ecosystem: implications for species at risk. For Ecol Manage 211:150−165

Vieira J, Campelo F, Nabais C (2009) Age-dependent responses of tree-ring growth and intra-annual density fluctuations of *Pinus pinaster* to Mediterranean climate. Trees (Berl) 23:257−265

Vieira J, Campelo F, Nabais C (2010) Intra-annual density fluctuations of *Pinus pinaster* are a record of climatic changes in the western Mediterranean region. Can J For Res 40:1567−1575

Wang H, Fu R, Kumar A, Li W (2010) Intensification of summer rainfall variability in the southeastern United States during recent decades. J Hydrometeorol 11:1007−1018

Xie L, Yan T, Pietrafesa LJ, Morrison JM, Karl T (2005) Climatology and interannual variability of North Atlantic hurricane tracks. J Clim 18:5370−5381

Zalloni E, de Luis M, Campelo F, Novak K and others (2016) Climatic signals from intra-annual density fluctuation frequency in Mediterranean pines at a regional scale. Front Plant Sci 7:579

Zhou Y, Matyas CJ (2017) Spatial characteristics of storm-total rainfall swaths associated with tropical cyclones over the eastern United States. Int J Climatol 37: 557−569

Editorial responsibility: Guoyu Ren,
Beijing, China

Submitted: April 16, 2019; Accepted: August 08, 2019
Proofs received from author(s): October 1, 2019